

Agricultural Crop Pattern Mapping and Change Analysis at a Sub-district Level Using Landsat satellite data: evidence from South-eastern Region, Bangladesh

BISWAJIT NATH^{1*}, MONIR HOSSAIN¹, SAHADEB CHANDRA MAJUMDER²

¹ *Department of Geography and Environmental Studies, Faculty of Biological Sciences, University of Chittagong, Chittagong-4331, Bangladesh*

² *Community Partnerships to Strengthen Sustainable Development Program (Compass), U.S. Forest Service, International Programs, Banani, Dhaka-1213, Bangladesh*

* *Correspondence details: nath.gis79@cu.ac.bd*

Submitted on: 2021, 31 August. Accepted on: 2022, 12 August. Section: Research Papers.

Abstract: The study first time identified and analyzed winter season agricultural crop patterns (ACP) derived from Land use (LU) maps in between 2010 to 2019 of south-eastern regions of Chittagong, Bangladesh. ACP identification was a challenging task in the worldwide research relevant to crop-related studies. To overcome this, we have considered frequently used traditional unsupervised classifier, such as K-means clustering algorithm technique. This has been applied on 30m pixel Landsat satellite reflectance images to identify crop pattern of the study area using the ENVI 5.3 and ArcGIS 10.8 software's, respectively. Multiple crops with seven classes were identified with the validation of in-situ ground-truth data and Google Earth (GE) images. The overall accuracy and kappa coefficient values were found at 81.96% and 0.79, respectively. The results suggest a significant variation of crop patterns in the study area and in recent time, the area largely dependent on mixed irrigation approach. Moreover, the crop pattern change was observed in the studied period as mixed crop 19% (9282.17 ha), Lentils (Pelon) 24.80% (11594.38 ha), Melon (Bangi) 22.37% (10461.08 ha), Chilis 17.90% (8367.48 ha), Paddy rice, unused land, and other crops, respectively. Among them, Lentils (Pelon) and Melon (Bangi) are identified as two common crops followed by mixed crops category, cultivated in the winter season as it required less irrigation compared to paddy rice area.

Keywords: *agricultural crop mapping; winter season; remote sensing; Landsat satellite; South-eastern region; Bangladesh.*

Introduction

Precise information delineation from satellite imagery at spatio-temporal scale is essential for assessing food security, management of agricultural resources, and regional sustainability of the area. However, the lack of monitoring of agricultural crop land (ACL) areas on a seasonal or annual basis for specific region wise is missing in the available literature. Therefore, it is crucial to focus on timely and accurate information about the extent and type of agricultural crops are planted in an area for yield estimation, food security assessment, agricultural inputs allocation and overall ecosystem sustainability.

Cropping pattern is a spatial phenomenon (Casasnovas *et al.*, 2005) which refers to the sequence and arrangements of crops in an area at a point in space and time. Timely information about cropping patterns and their change is a prerequisite to devising an ideal pattern within an agro-ecological region (AEZ). Remote sensing and Geographical Information System (GIS) has become very effective tools for the management of dynamic agricultural resources (Ray *et al.*, 2005; Nellis *et al.*, 2009; Liaghat and Balasundram, 2010; Santanu *et al.*, 2014). The integration of remotely sensed data and GIS techniques have been extensively used in the cropping pattern change analysis, optimal land use planning, and precision of agriculture (Odenweller and Johnson, 1984; Pradhan, 2001). Satellite imagery has made it possible to map and monitor croplands with high spatial resolution (Panigrahy *et al.*, 1995; Foley *et al.*, 2011; Yu *et al.*, 2013; Fritz *et al.*, 2013; Lie *et al.*, 2016; Tian *et al.*, 2018) and identify crop types at local, regional and global level (Quarmby *et al.*, 1992; Wu *et al.*, 2015; Wang *et al.*, 2019).

Monitoring agricultural production requires routinely updated information on the total surface under cultivation, where crops were considered as an input (Justice and Becker-Reshef, 2007; Ozdogan, 2010; Atzberger, 2013). Therefore, accurate and effective method is essential to map and monitor the distribution of agricultural lands and its different crop types (Panigraphy and Sharma, 1997; Liu *et al.*, 2016; Wang *et al.*, 2019). Several popular image classification parametric and non-parametric methods such as Unsupervised K-means clustering, and ISODATA (Mingwei *et al.*, 2008; Singh *et al.*, 2011; Belgiu *et al.*, 2021), Supervised Maximum Likelihood classifier (Feng *et al.*, 2019; Mingwei *et al.*, 2008) and Random Forest (RF) and Support Vector Machine (SVM) from machine learning (Feng *et al.*, 2019), respectively are widely used in crop mapping and change analysis.

Contrarily, satellite remote sensing data analysis is a cost-effective way to generate up-to-date crop classification maps for larger areas at various scales (Murakami *et al.*, 2001; Wardlow and Egbert, 2008; Wardlow *et al.*, 2007; Conrad *et al.*, 2010; Thenkabail, 2010; Panigraphy and Sharma, 1997; Long *et al.*, 2013; Li *et al.*, 2015; Waldner *et al.*, 2015; Wu *et al.*, 2015). Crop mapping on a regional scale, i.e., larger than 1000 km² using 10-30m spatial resolution multispectral remote sensing satellite data is still the preferred choice of the scientific communities across the world (Waldhoff *et al.*, 2012; Liu *et al.*, 2005). Further, when it used in continuous monitoring purposes in all seasons based, it reveals specific atmospheric problems such as cloud interference over satellite scenes, especially in tropical and sub-tropical regions across the globe. In addition, seasons (i.e., winter/summer crops) and weather conditions are varied with different crop development may hinder the crop pattern differentiation at regional or local scales (Whitcraft *et al.*, 2015). Therefore, by observing the problems in other studies, specific season such as winter (December to March)

is found almost clear within our study area and Landsat satellite scenes are available with less percentage of cloud cover during this time compared to other seasons. Multi-year and multiple crop pattern mapping (Singh, 1980; Casasnovas *et al.*, 2005; Singh, 2011; Jain *et al.*, 2013; Garcia *et al.*, 2019), specific crop identification (Nasim *et al.*, 2017) and area estimation was still lacking in developing countries, especially at sub-district level in Bangladesh.

To maintain sustainable agricultural growth of a country and food security at national, and international level, sub-districts wise agricultural crop pattern (ACP) mapping is extremely essential when a country like Bangladesh is lacking at local and regional level accurate agricultural statistics. In Bangladesh, agricultural statistics yearbook is published in a district and divisional basis in a particular year with lack of detail ACP information. Therefore, sub-district (local unit: *Upazila*) level ACP identification, mapping and accurate estimation is necessary to attain regional crop production and ecological sustainability of the study area.

In addition, to support the growing number of populations food demand, PRC areas have faced a critical challenge in different seasons, which forces the local cultivators towards the multiple crop practices. In recent, Shahidullah *et al.*, (2017), were observed the changes in multiple crop practices over 42 Upazilas of Chittagong region in 2016 using pre-tested semi-structured questionnaire with a specific view to document the existing cropping patterns, cropping intensity and crop diversity. Moreover, Rahman and Saha (2009) conducted study in Bogra district (western part of Bangladesh) to map seasonal crop land considering Landsat TM, and IRS P6 LISS-3 satellite images from 1988/89 to 2004/05 time periods using object-based classification. However, in recent, LULC changes was observed in transformation of significant parts of the Hathazari Upazila and its quantitative assessment from 1977-2017 using Landsat MSS, TM and OLI satellite imageries (Bhuiyan *et al.*, 2019).

Till date, study on crop pattern mapping at sub-district level considering Landsat satellite data is still missing in our study areas. A long-term Landsat satellite datasets with 30m resolution might be a good choice for the sub-district level agricultural crop change assessment. Moreover, in recent time, study areas have faced some critical physical challenges during crop practices in winter seasons compared to other seasons, because of non-availability of water during this time. As a result, farmers of two sub-districts areas (i.e., Hathazari, and Raozan Upazila) have shifted in multiple crop practices. By observing this, the present study particularly moving forward with specific research questions: such as, (a) what type of crops are practice in recent year compared to earlier? (b) which crops are mostly transformed to another practices during winter time? and (c) how much areas have changed in recent compared to earlier?. Therefore, to solve these questions, the present study is considered as a first kind of attempt in the south-eastern region of Bangladesh aimed at identifying agricultural crops (AGC) such as, Lentils (Pelon), Melon (Bangi), Chilis, mixed crops, which practiced in winter season from 2010 to 2019 time period. By knowing this, the ACP maps, historical and current changing status and corresponding digital databases will be considered as a good baseline data source for the sustainable agricultural practices in this area.

However, the specific objectives of this study are: (a) to identify crop patterns of the study area that undergone changes since 2010 to 2019; and (b) to map spatio-temporal variations of ACP, and its statistical comparison in four-time domains as 2010, 2014, 2018 and 2019; and (c) to analyze the ACP dynamics, persistence and changes in agricultural practices based on three-time intervals (2010-2014, 2014-2018, and 2018-2019) through Sankey diagram.

Materials and Methods

Study area

The two sub-districts (Hathazari and Raozan Upazilas) of Chittagong district were considered in the present study, which lies between latitudes 22°37'N to 22°40'N and 91°42'E to 91°59' E longitudes of the southeastern region of Bangladesh (Fig. 1). It covers an area of 46772 hectares, where Hathazari and Raozan Upazila shares 22802 hectares and 23970 hectares, respectively, and is bounded by Fatikchhari Upazila in the north-east, Chittagong City Corporation (CCC) in the south, and Sitakunda Upazila in the west. The selected both Upazilas are considered as one of the important crops producing zones in the district of Chittagong, Bangladesh which having practiced and cultivated by many agricultural crops round the year. The study areas are geographically considered as high to medium high land categories (Brammer, 1996) and situated in 23 (Chittagong Coastal Plain) and 29 (Eastern Hills) Agro-ecological Zones (AEZ) of Bangladesh (Huq and Shoab, 2013).

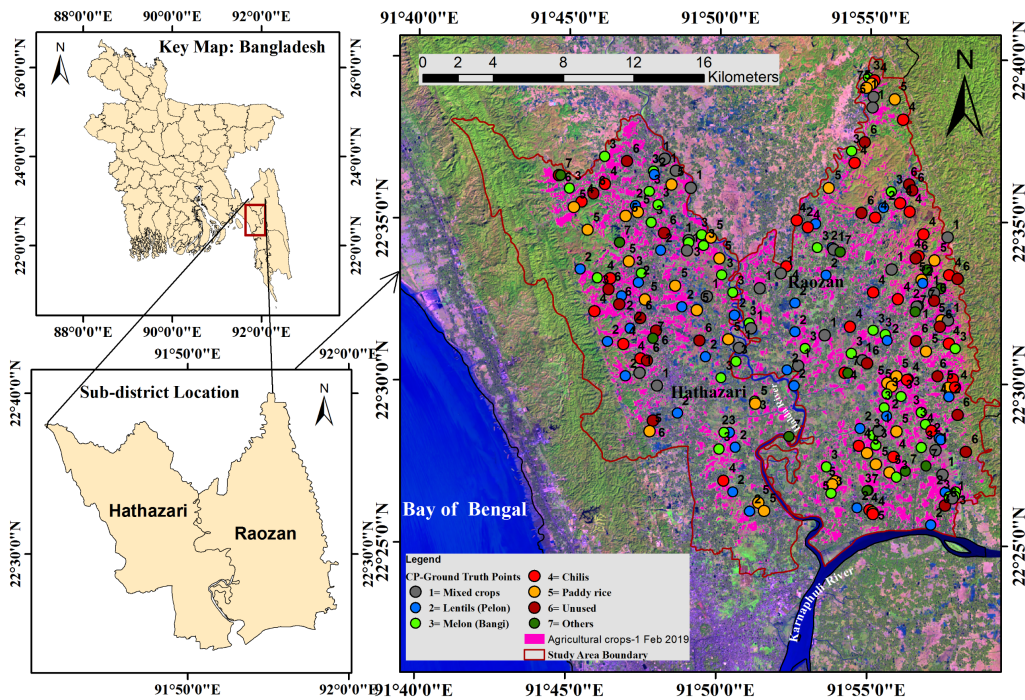


Figure 1: Location of the study area in South-eastern region, Bangladesh

The maximum and minimum temperature ranges are 25-37°C and 10-21°C, respectively. The annual average rainfall is 2590 mm, and the general soil condition is clay loam to sandy loam (Huq and Shoab, 2013). In addition, the time series, area averaged of average surface skin temperature (GLDAS model, 0.25 deg. resolution, daily, unit in kelvin converted to

degree Celsius) and precipitation (TRMM_3B42 daily, unit: mm/day) is shown in Fig. 2. The major crops grown in this area are Lentils, Melon, Chilis, Paddy Rice, etc.

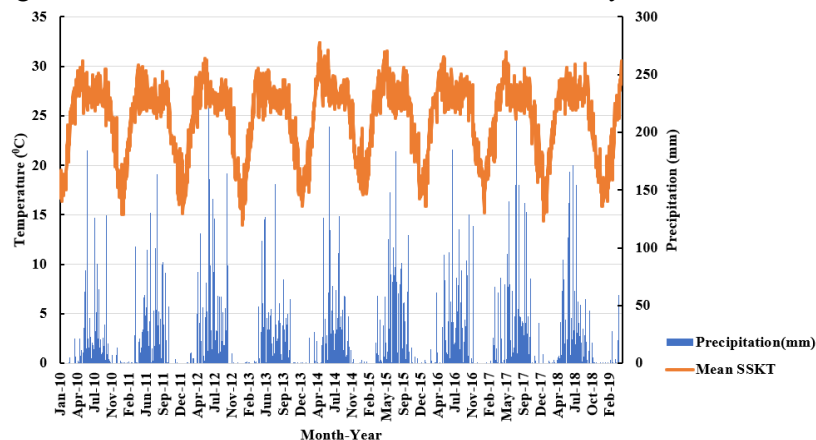


Figure 2: Time series area averaged of daily mean surface skin temperature (SSKT) and precipitation in the study area

Data collection

To achieve the aims of the study, both primary and secondary data were collected from multiple sources. The primary data sources involved farmers/land owners' interview, direct field observation and global positioning system (GPS) survey, field photos by digital camera, and high-resolution Google earth (GE) pro images. GE pro images were collected before primary field visit based on study area boundary vector layer (i.e., GIS shapefile of Hathazari and Raozan Upazila administrative boundary) including country boundary were collected from the freely available WFP (World Food Programme) website (<https://geo.node.wfp.org>). This shapefile then converted into kml to open in GE pro platform, which helps us to acquired images and its further uses in the field survey to identify LU category and ACP information.

Moreover, multi-spectral Landsat satellite imageries were collected as the initial secondary data source. Besides this, other secondary data such as Environmental System Research Institute (ESRI) provided World Wayback imageries in three different times (31 January 2019, 14 December 2018, and 20 February 2014) (as close to satellite dates) and January 2010 from GE pro were considered as reference images in this study.

In addition, different relevant publications, government agricultural statistics year book from 2010-2019 and other processed ready data of precipitation and temperature were accessed and considered in this study. The details of satellite and ground data collection and its uses are described in the following two sub-sections.

Satellite data collection

Landsat satellite images having two different sensors (i.e., Landsat-5 Thematic Mapper (TM) and Landsat 8 Operational Land Imager (OLI) with 30m resolution were downloaded from the United States Geological Survey (USGS) Earth Explorer Archive (<https://earthexplorer.usgs.gov>). These two sensors' images were used for visual image interpretation, LU classification, ACP identification from agricultural crop land derived from LU classes, spatial distribution and change analysis.

As the changes happened in the study areas due to increasing trend of populations and extensive utilization of land, the farmers have slowly shifted toward multiple crop practices and it may vary from season to season in a single year. The changes are severe in winter season due to non-availability of water. Therefore, winter season of the year 2018–2019-time span was preferred in the present study for initial screening of ACP in the study area. To investigate the ACP at field level, the survey period extended from March–April 2019, but unfortunately the image is covered by cloud, thus, image selection time was considered till the month of February, as the particular image is cloud free. The other three Landsat satellite data sets i.e., 2018, 2014, and 2010 were considered to observe the past ACP status as farmers in both areas confirmed that their crop practices shifted since 2010. Therefore, the study confirmed the image selection periods from that time at 4 years interval (such as, 2010, 2014, 2018) to compare with the recent one as on 1 February 2019. The details of satellite data specification are shown in Table 1.

Table 1: The satellite datasets used in the study

Satellite sensors	Date of acquisition	Path/row	Resolution (m)	Band used	Scene cloud cover (%)
Landsat -5 TM	23 Jan 2010	136/44	30	Multispectral	1.00
Landsat -8 OLI	2 Jan 2014	136/44	30	Multispectral	0.06
Landsat -8 OLI	31 Dec 2018	136/44	30	Multispectral	0.00
Landsat -8 OLI	1 Feb 2019	136/44	30	Multispectral	0.06

Ground data collection

To mark on high resolution GE images, ground truth point's (GTP) data was collected in two separate ways such as, for generalized LU categories and agricultural crop types. These data are recorded as coded information in the field notebook along with Global Positioning System (GPS) coordinates. Total 150 GTP considered for the LU (see supplementary Fig. 1) and 212 points for ACP identification (see Fig. 1) were collected through Garmin handheld E-Trex GPS receiver during March–April 2019 used as GTP. The GTP shape file are integrated in the geographic information system (GIS) database. The code is a numeric value (1-5) for LU (see supplementary Fig. 1 for code details) and (1-7) for ACP assigned in this study (Fig. 1). The ACP codes and number of GTP collected according to multiple crop types is shown in Table 2.

We used field data for classifying year 2019 crops and for the rest historic years used understanding of 2019 year's field data. To be more precise, we prepared color pallet of each crop type using 2019 data in the ESRI Wayback (<https://livingatlas.arcgis.com/wayback/>) imagery (see supplementary Fig. 2 as sample reference image) and Google Earth (GE) imagery. As the year 2018, 2014, and 2010 lack GTP, we further use those color pallets overlaying with Wayback imageries and GE imageries along with expert judgement, we have drawn the training samples of the years 2018, 2014, and 2010. The image time frame we considered in this study which back to the 2010, as farmers in both areas have confirmed that they have started practices of different crops since then. The representative field photos of the selected ACP along with coordinates of each crop type was collected through digital camera and GPS survey, respectively. The validation points were generated in the field data before running the classification, and two groups of points were separated of which one set for training the classification and another set for result validation. The comparison results of ground truth is shown in Table 2.

Table 2: Number of points collected at field level for each ACP identification in the study (codes are assigned for ACP)

ACP Code	ACP Classes	Ground Truth (2019)	Classified Validation (2019)	Classified Validation (2018)	Classified Validation (2014)	Classified Validation (2010)
Code-1	Mixed crops	26	27	27	23	27
Code-2	Lentils (Pelon)	38	37	37	38	36
Code-3	Melon (Bangi)	50	42	44	46	44
Code-4	Chilis	32	30	29	33	32
Code-5	Paddy rice	28	30	30	27	35
Code-6	Unused	28	30	30	32	25
Code-7	Others	10	16	15	12	13
	Total	212	212	212	212	212

Methodology

K-Means clustering and ISODATA algorithm classification approach were used for crop types identification (Hong et al. 2014) and several other studies have reported the advantages of applying unsupervised classification methods on multi-source data (Okamoto 1999; Hill et al. 2005; Hong et al. 2011, 2014). Therefore, in this study, we have considered frequently used traditional K-means clustering unsupervised image classification approach in the data gap regions focusing for the first time at sub-districts level crop mapping exercise. This has been especially considered to know the crop types, distribution and temporal changes. The methodological workflow is shown in Fig. 3 followed by the details of breakdown of its multiple steps (sections 2.3.1 to 2.3) are discussed in a systematic manner.

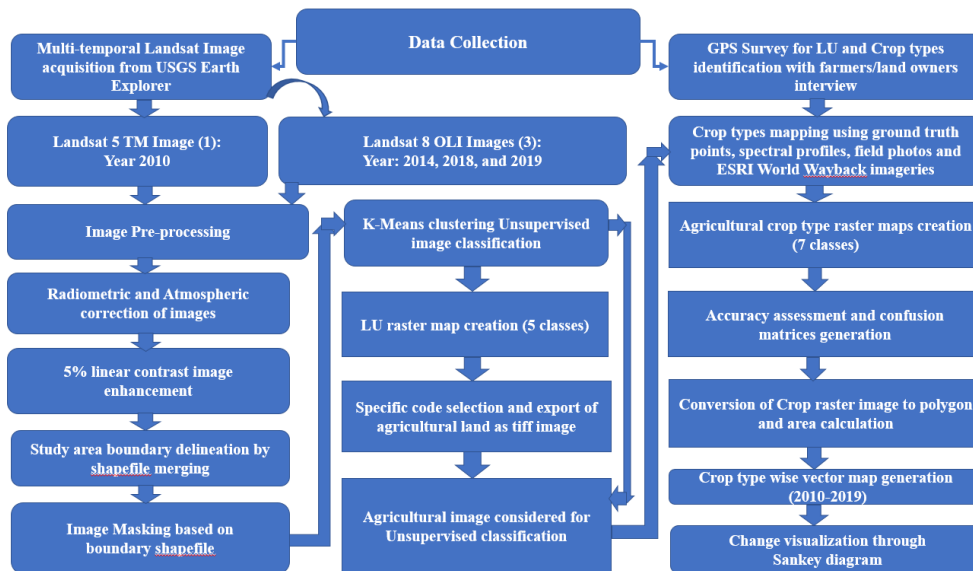


Figure 3: Flow chart of the methodology used in this study

Pre-processing of satellite imageries

The Landsat archive collected imageries need to be pre-processed before derive any useful information which need to go through several steps. For radiometric correction, each multispectral image raw DN value was converted into Top of Atmosphere (TOA) reflectance

image, and then adopted Dark Object Subtraction (DOS) method in ENVI 5.3 software, to get atmospheric corrected image. The corrected reflectance images were then applied 5% linear contrast enhancement for better visualization and initial stage image interpretation. In the next step, all multispectral bands for the respective sensors images for the particular year was considered for digital image interpretation and classification. In the final step, shapefile of two sub-districts (Hathazari-Raozan administrative boundary) were merged together to form an overall study area boundary, which finally used to image masking of the respective year reflectance images.

Image classification process, class labelling and accuracy assessment method

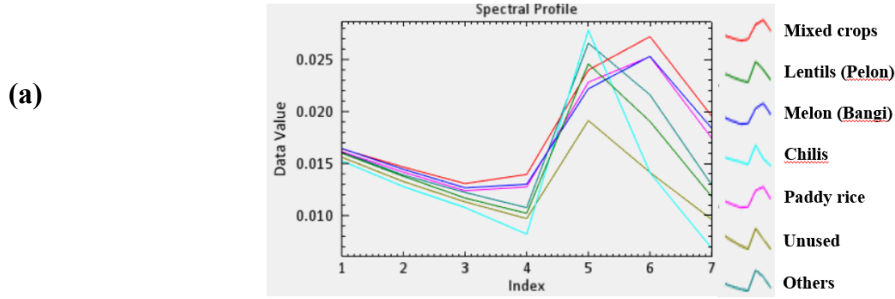
The atmospheric corrected reflectance images were considered in image classification. Unsupervised K-means clustering classification technique was used in both LU and ACP classification. For general LU classification, the total number of classes were considered five, and in ACP classification it was considered seven classes. The default parameters value within K-means parameters window under classification workflow of ENVI 5.3 software was considered for unsupervised classification. K-means parameters is found robust in this regard, as it correctly classified and verified with the aid of field GPS along with high resolution GE images and ESRI World Wayback imageries. To accurately compute the area of different types of LU, the specific geographic projection information (UTM projection with zone 46N) was assigned on each image. At this stage, each classified image of LU has been used for classification accuracy assessment and error matrices calculation. Then, from LU category, agricultural land was queried based on its code available from attribute table. This has been exported further into tiff image by using ArcGIS 10.8 software, later imported in ENVI 5.3 environment for unsupervised classification to identify multiple crop types of the study area.

The specific ACP identified initially at the field level by following simple random sampling method with the farmers/land owner's opinion regarding their crop practices at present and earlier times. The seven ACP codes and its label such as, Code-1= Mixed crops, Code-2= Lentils (Pelon), Code-3= Melon (Bangi), Code-4= Chilis, Code-5= Paddy rice, Code-6= unused, Code-7= others were used to mark on GE images along with corresponding ground truth GPS coordinates (see Table 2) of particular agricultural crop types. To support image classification, ground truth GPS coordinates are used for 2019 image accuracy assessment. The classified images of 2018, 2014, and 2010 are validated with the random point's creation (see Table 2 for each year classified validation points) in the same location points of 2019 using ArcGIS 10.8 software in support with the reference's images of ESRI World Wayback imageries of 14 December 2018, and 20 February 2014 and 31 December 2009 image from GE pro.

The following conditions were followed during coding stage, such as, If the corresponding class match each other, code it allocated as same (for example, code=1 is equal to code =1), and if not match each other on classified image, the representative class category is identified as different class.

The corresponding spectral signatures of multiple crops (Fig. 5a) are derived from image pixel (30m resolution) after verification with corresponding field GPS coordinates. Here, for example, Landsat 8 OLI 2019 reflectance image bands from 1 to 7 (referred as, Coastal aerosol, Blue, Green, Red, Near-Infrared, SWIR1, and SWIR2, respectively) were displayed as reference signatures. In addition, the confusion matrix and accuracy assessment tables

were generated based on the multi-temporal crop images (i.e., 2010, 2014, 2018, and 2019, respectively) as given in the sub-section 4.3. To understand the previous crop practices at the same pieces of land, we have depended on farmer's opinion and their previous understanding, therefore, accuracy of the earlier crop's classifications is less compared to recent time.



Spectral profiles of seven agricultural crop categories derived through generating random points on Landsat 8 OLI reflectance image (1 Feb 2019)

(b)

Field photo	GE image	Field photo	GE image
			
(b) Mixed crops	(c) Mixed crops	(d) Lentils (Pelon)	(e) Lentils (Pelon)
			
(f) Melon (Bangi)	(g) Melon (Bangi)	(h) Chilis	(i) Chilis
			
(j) Paddy rice	(k) Paddy rice		

Figure 4: (a) Spectral profiles of various types of crops (seven classes) and (b,d,f,h,i) Field photos of major crops and (c,e,g,i,k) GE images of corresponding class

The classification results were produced and compared based on the established formula adopted by (Congalton, 1991; Congalton and Green, 2008; Islam *et al.*, 2018) useful to assess user's accuracy, producer's accuracy, overall accuracy, kappa coefficient values and errors of commission and omission (Cohen, 1960) for the classified image. The widely used formulas considered for overall accuracy assessment are calculated from the error matrix using Equations 1-3.

$$K^{\wedge} = \frac{P_o - P_e}{1 - P_e} \quad (1)$$

$$P_o = \sum_{i=1}^r P_{ii} \quad (2)$$

$$P_e = \sum_{i=1}^r (P_{i1} * P_{i2}) \quad (3)$$

where r is the number of rows in the error matrix, P_o is the proportion of observed agreement, P_e is the proportion of agreement expected by chance, P_{ii} is the proportion of pixels in row 'i' and column 'i', P_{i_1} is the proportion of the marginal total of row 'i', and P_{i_2} is the proportion of the marginal total of column 'i'.

Spatial data query, crop type's distribution and change analysis method

The classified ACP raster images from four different years were converted to vector files with the conversion tool box of ArcGIS 10.8 software (ESRI, USA). Further, the vector file is used to calculate ACP area statistics by year and Structured Query Language (SQL) commands such as Select by attribute and Select by Location query were used to extract spatial distribution data by crop type. In this regard, the 2019 reference is displayed as a syntax which is used to calculate the total area of individual crops by the Auto-SUM option. By following this, rest of the year's crop area is calculated. The SQL query syntax which represented for the year 2019 is shown below:

```
Select by attribute > Layer: CP_1 Jan 2019 > Method: Area_Hec >  
Select * From CP_1 Jan 2019 WHERE: "gridcode" =1 > Apply > OK
```

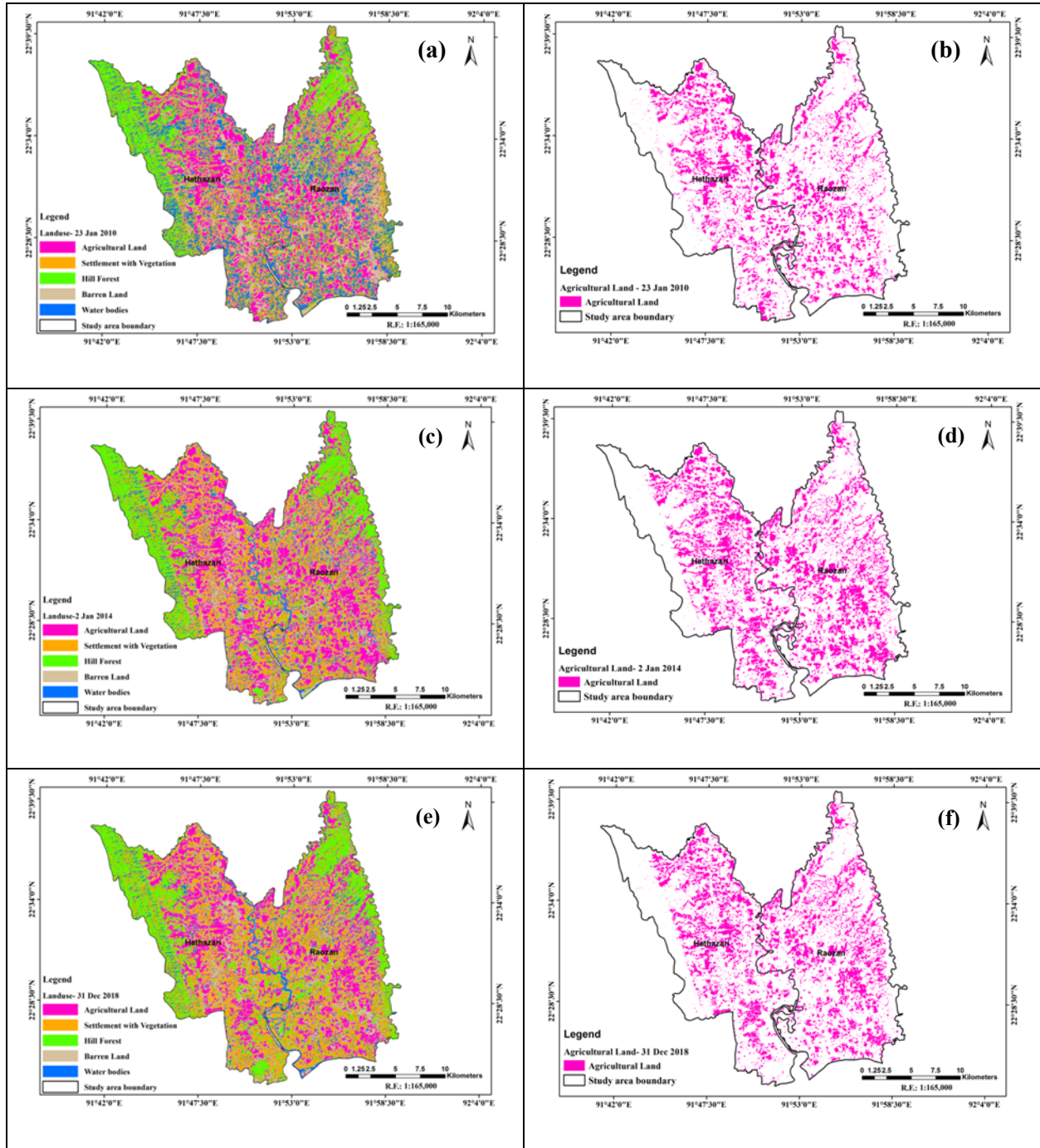
The corresponding statistics are collected and systematically arranged in a table for further analysis. Spatial distribution of individual crop map is prepared and exported to shapefile for final visualization. The crop type statistics of four years is tabulated and further used to assess the change, percentage of change and annual rate of change by following three equations 4-6.

$$\text{ACP change} = \text{Magnitude of the New Year} - \text{Magnitude of the Previous Year} \quad (4)$$

$$\text{Change(\%)} = \text{Magnitude of change} * 100 / \text{Base Year} \quad (5)$$

$$\text{Annual rate of change(\%)} = \text{Final year} - \text{Initial year} / \text{No. of Years} \quad (6)$$

In the next, the corresponding information of total number of individual crop field patches (TNCFP) and mean crop field patch size (MCPS) (area in hectare) are calculated by spatial attribute query and statistical summation (Σ) option within the ArcGIS 10.8 software. The corresponding data are then used for graphical representation. Moreover, the vector files were used in change transformation analysis for the three-time periods such as, 2010-2014, 2014-2018, and 2018-2019. Finally, the ACP dynamic change flow from one class to another is prepared based on the Sankey diagram, which is a powerful visual displaying, dynamically edited, simple and intuitive interface program and add-in tools supported in MS Excel by Power-user software (<https://www.poweruserssoftwares.com>).



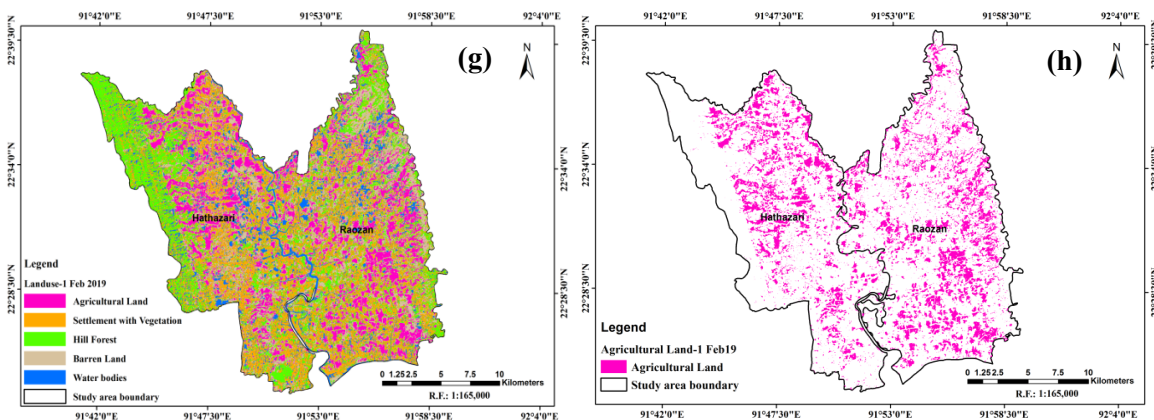


Figure 5: LU maps and resultant spatio-temporal distribution of agricultural land of the study area from 2010-2019. (a) LU map- 23 Jan 2010; (b) agricultural land- 23 Jan 2010; (c) LU map- 2 Jan 2014; (d) agricultural land- 2 Jan 2014; (e) LU map- 31 Dec 2018; (f) agricultural land- 31 Dec 2018; (g) LU map- 1 Feb 2019; (h) agricultural land- 1 Feb 2019.

Results and Discussions

Landsat-derived LU mapping and analysis from 2010 to 2019

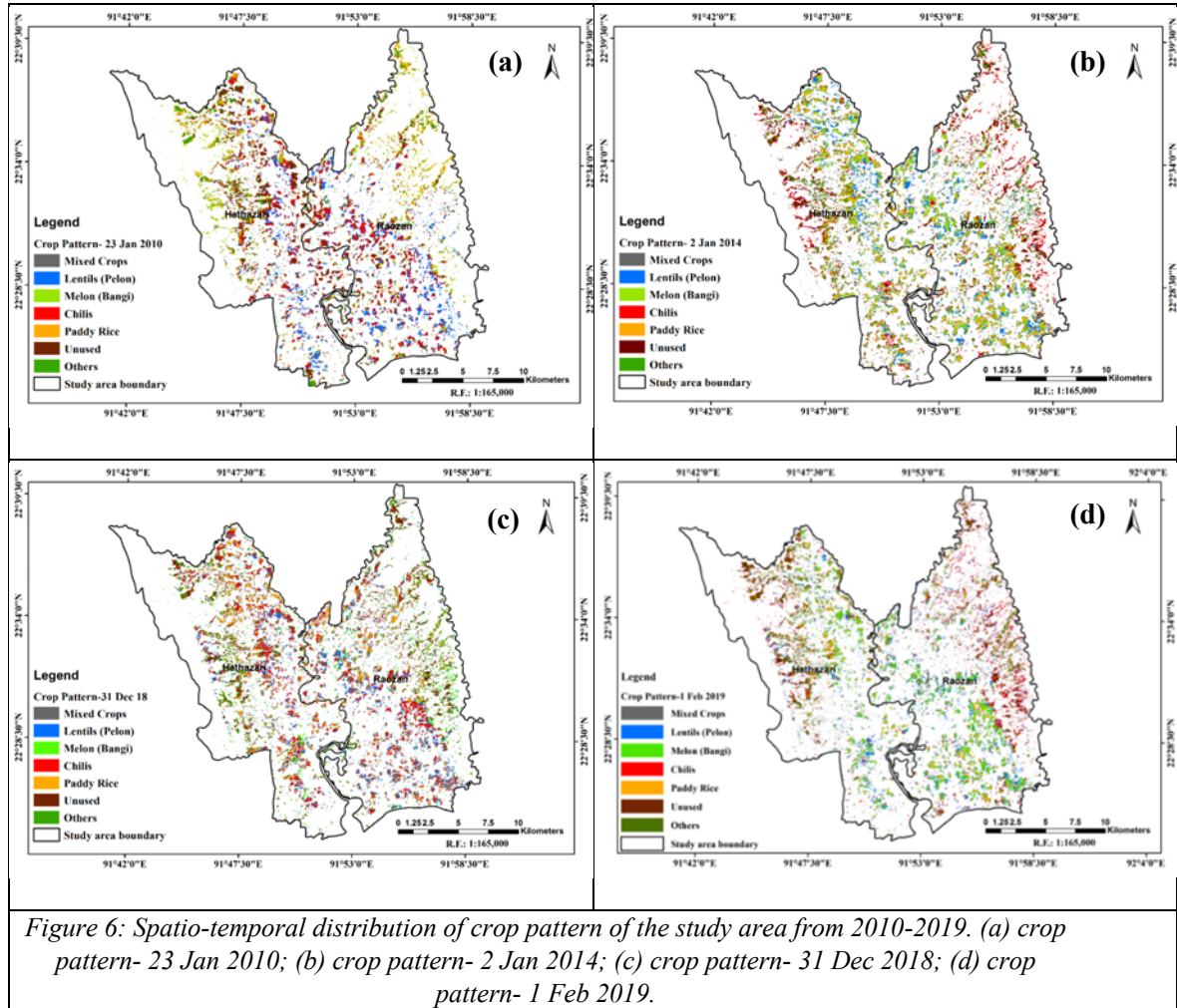
The different LU pattern of the study area from 2010 to 2019 is displayed in Figs. 5(a,c,e,g). The present LU of five major categories e.g., (a) agricultural land, (b) settlement with vegetation, (c) hill forest, (d) barren land, and (e) water bodies are identified at two sub-district level (Hathazari and Raozan upazila) based on the method discussed in section 3.2.2. The agricultural land and their spatio-temporal distribution maps were presented in Fig. 5 (b,d,f,h). All the maps in this study are prepared on 1:165,000 scale in the ArcGIS 10.8 software environment (Figures 5a-h). The details information of LU area, spatial distribution (in %) based on total area along with temporal change statistics were calculated and presented in supplementary Table A.1. The total area of the study area is 46757.45 ha.

From the identified LU categories, settlement with vegetation was the most dominant LU category identified in the study area and its share is 25.24%, 29.31%, 31.17% and 30.21% in 2010, 2014, 2018 and 2019, respectively (Figs. 5a, c, e, g and Table A.1). On the other hand, Agricultural land shares 19.85%, 24.80%, 22.37%, 17.90% in the same time periods as mentioned above (Figs. 5b, d, f, h and Table A.1). The major shares of this land are mainly concentrated in north and north-west of Hathazari and south and south-east of Raozan Upazila. Moreover, during field investigation, farmers confirmed that they are less interested in paddy rice crop cultivation in winter season. As a result, more areas were left as barren land with an increasing trend of 23.22% observed in 2019 compared to 21.92% in 2010 (Table A.1).

Spatio-temporal distribution of multiple crops from 2010 to 2019

In this study, we have derived ACP and its statistics based on the method discussed in Section 3.2.3. To observe this spatio-temporal variations, we have selected the time frame at 10 years (from 2010 to 2019) for our study. Based on the all-temporal CP images (Figs. 6a-

d), the proportion of Mixed crops (such as Pumpkin, Tomato, Cabbage and Cauliflower) areas at two sub-district level increased in recent time 11.59% in 2019, compared to 4.59% in 2010. The spatial distribution of mixed cropping culture is dominated only in the north, north-western part of Hathazari, whereas it is concentrated in north, north-eastern part of Raozan Upazila. These concentrations were shifted towards the direction, where earlier Chilis, Melon (Bangi), Paddy rice and others cropping areas were located.



The crop types dynamic distributions in four times (i.e., 2010, 2014, 2018, and 2019) defined by seven crop types are calculated based on the unsupervised classified results which is shown in Table 3.

Table 3: Category wise Crop type's distribution in the study area from 2010 to 2019.

ACP CATEGORIES	2010		2014		2018		2019	
	AREA (HA)	AREA (%)	AREA (HA)	AREA (%)	AREA (HA)	AREA (HA)	AREA (HA)	AREA (HA)
Mixed Crops	426.84	4.59	594.80	5.13	1448.13	13.84	970.47	11.60
Lentils (Pelon)	1985.83	21.39	2326.75	20.07	1749.75	16.73	1431.83	17.11
Melon (Bangi)	1476.75	15.91	2761.75	23.82	1263.20	12.08	1880.87	22.47
Chilis	2117.35	22.81	1377.10	11.88	2091.68	19.99	1200.34	14.34
Paddy Rice	1039.11	11.20	1878.92	16.20	1524.27	14.57	1077.29	12.88
Unused	1330.84	14.34	1550.84	13.38	1421.51	13.59	1076.58	12.87
Others	905.45	9.76	1104.22	9.52	962.70	9.20	730.50	8.73
Total	9282.17	100	11594.38	100	10461.24	100	8367.88	100

Source: USGS Landsat satellite data-based cropland information from 2010 to 2019 and data computed by authors.

Among all the categories, the total area of Chilis_{Landsat-8} cultivation in 2019 sharply decreased to 14.34% (1200.34 ha) in 2019, which was 22.81% (2117.35 ha) (as the top shares) in 2010_{Landsat-5} among all the available crop types (Table 3). However, both the study regions had also higher percentage of shares of Lentils (Pelon)_{Landsat-5} 21.39% (1985.83 ha) and Melon (Bangi)_{Landsat-5} 15.91% (1476.75 ha), and paddy rice_{Landsat-5} 11.20% (1039.11) cultivation in the year 2010. The shared of Lentils (Pelon) sharply reduced after 2010_{Landsat-5} which continued till 2019_{Landsat-8} (Table 3). The two crops such as, Melon (Bangi) and Chilis have followed the trends like decrease-increase-and further decreasing trend in both the areas. On the other hand, the Paddy Rice_{Landsat-8} cultivation share is slightly increased (12.88%) in 2019 (Table 3 and Fig. 6d) compared to 11.19% in 2010_{Landsat-5} (Table 3 and Fig. 6a).

Accuracy assessment based on image classification results

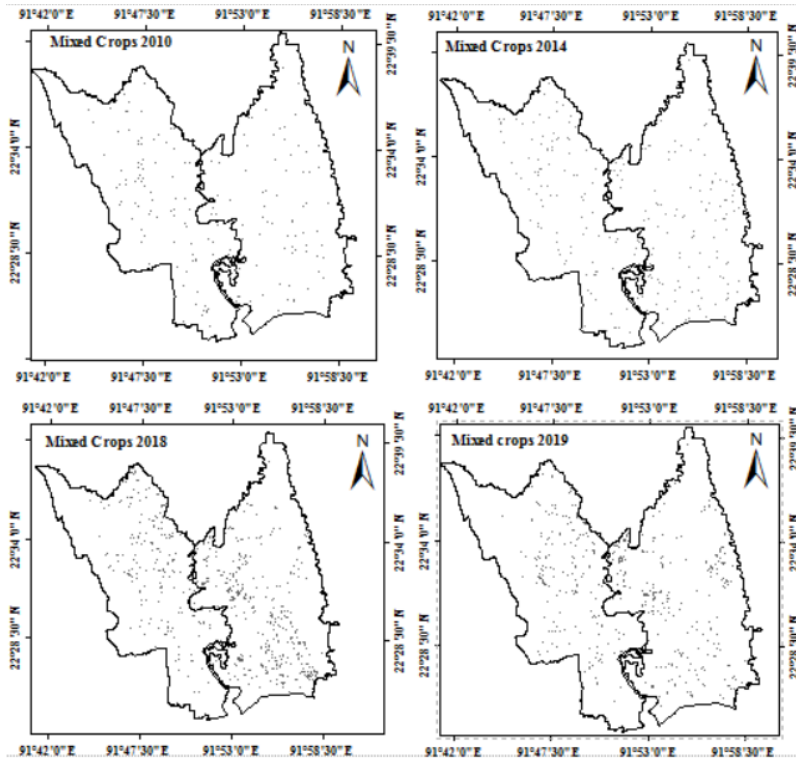
The accuracy assessment of the multiple years (i.e., 2010, 2014, 2018, and 2019) LU maps were conducted at the initial stage based on the unsupervised classification maps with randomly generated points and ground truth field validated points (in total 150 points) (see appendix B: supplementary file Fig. 1). The overall accuracies for LU were achieved 76.67%, 74.67%, 71.33%, and 82.00% in 2010, 2014, 2018, and 2019, respectively; while the Kappa coefficients were 0.70, 0.67, 0.63, and 0.77, respectively based on the Eq. 1-3 (shown in Section 3.2.2). The details of crop type classification accuracy and confusion matrices in four different years have shown in appendix Table-B (a-d).

The validation results showed the others category in 2019 has a reasonably high accuracy in this year map followed by Paddy Rice 90.62% producer accuracy (PA), 89.29% user accuracy (UA) and Mixed crops 88.46 PA, 85.18% UA (Appendix Table-B: d). In comparison, Melon (Bangi) in year 2014 had a higher accuracy with 97.03% PA and 97.03% UA than all remaining crops identified in that year (Appendix Table-B: b). However, in 2018, Chilis had a high level of accuracy with 87.50 PA and 96.55% UA (Appendix Table-B: c). Among all four years, the UA and PA of the important major classes (i.e., Mixed crops, Lentils, Melon, Chilis and Paddy Rice) were observed within the range of 66.67-97.83% and

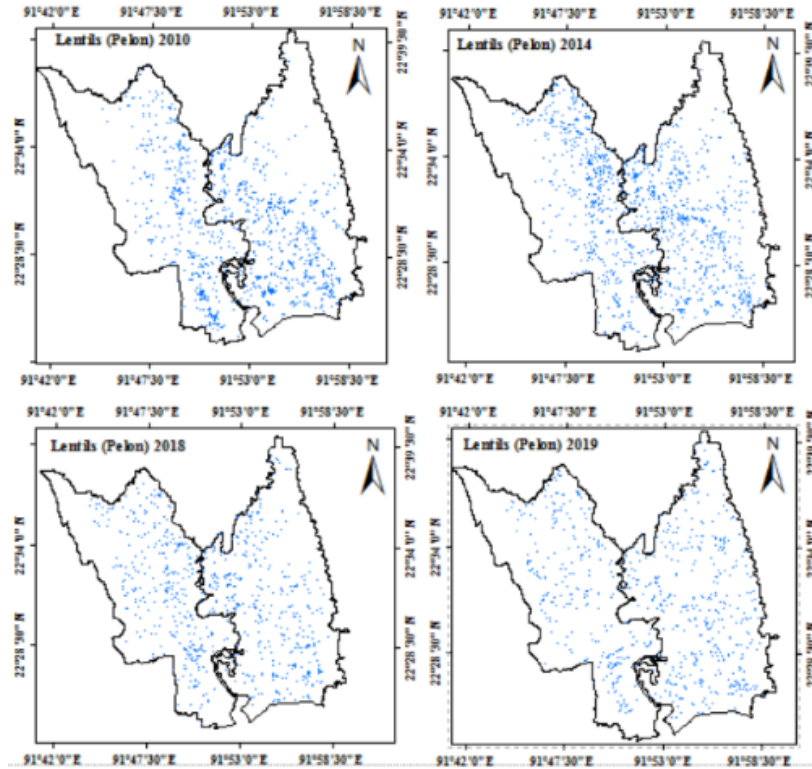
87.50-96.55%, respectively. The overall accuracies and the Kappa coefficients in the CP are 81.13%, 86.79%, 76.89%, 83.02% and 0.78, 0.84, 0.73, and 0.80 in 2010, 2014, 2018, and 2019, respectively (Appendix Table-B: a-d). Unfortunately, due to absence of crop related published works, the results derived from this study is difficult to compare.

Spatial distribution of Crop pattern change analysis of the study area (2010 to 2019)

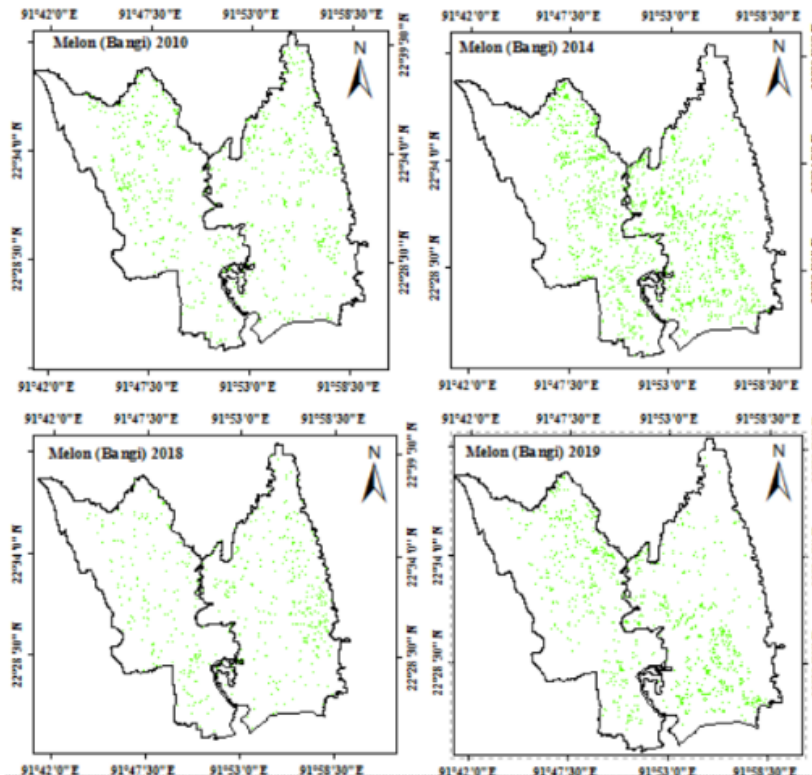
The spatial distribution of class-wise changes of ACP in the study area from 2010 to 2019 are presented in Figs. 7(a-g). The corresponding crop area statistics are demonstrated in hectares and percentage is already shown in Table 3 (see section 3.2).



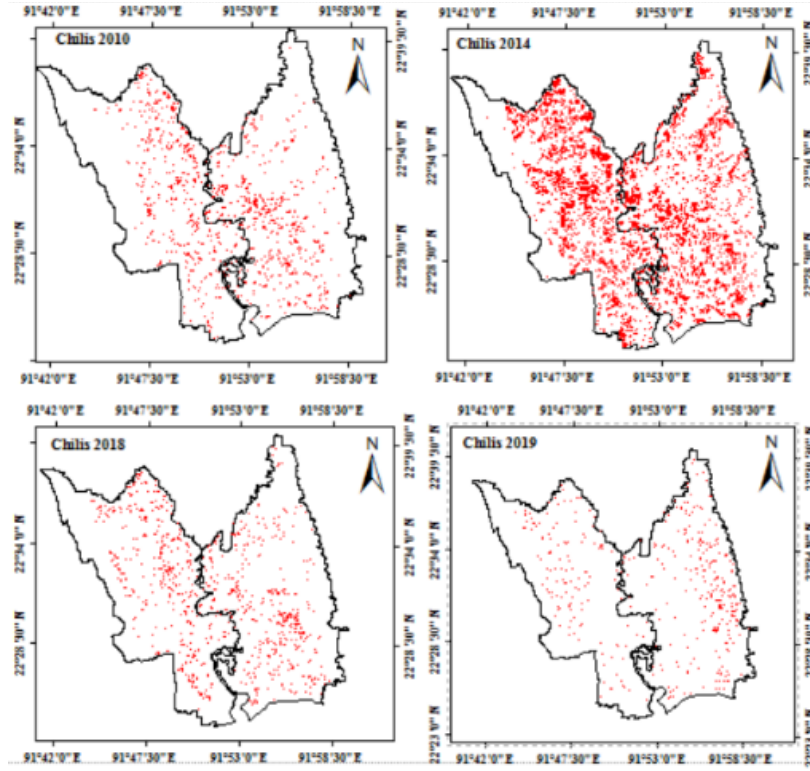
(a)



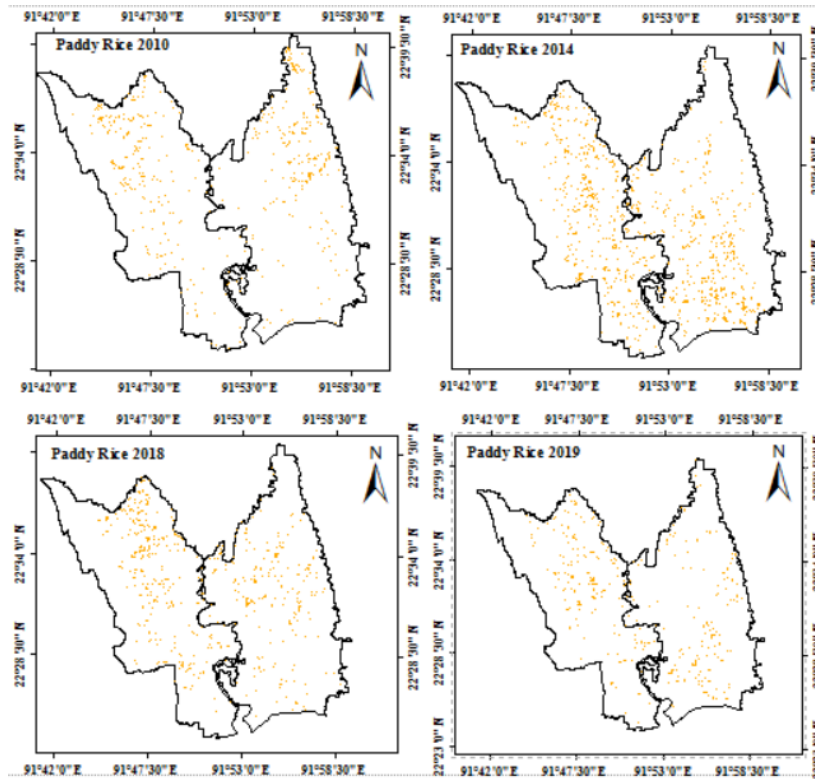
(b)



(c)



(d)



(e)

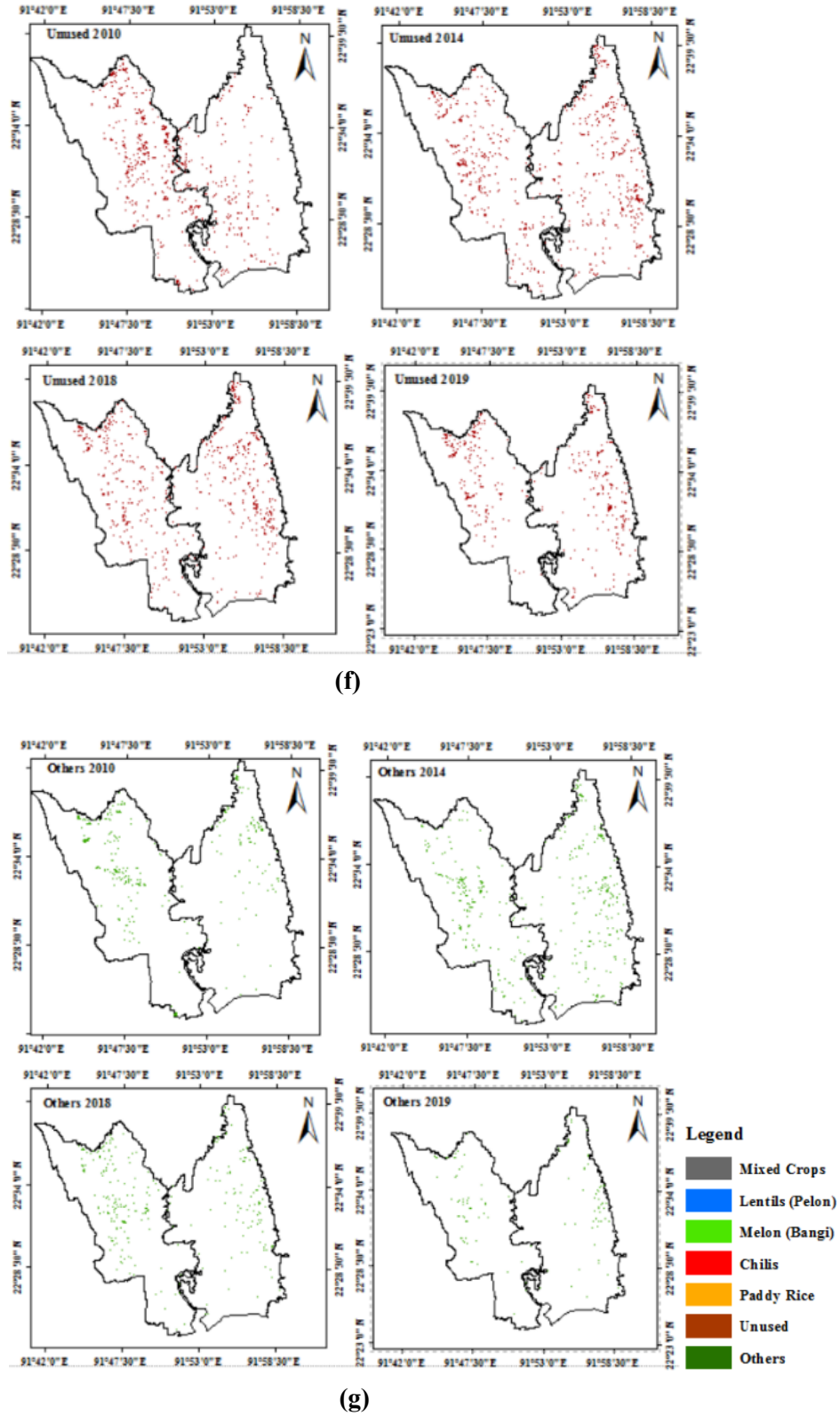


Figure 7 (a-g) - Spatial distribution of class wise changes of ACP in the study area from 2010 to 2019

Crop field patches and Mean patch sizes estimation of the study area from 2010 to 2019

The total number of field patches (TNFP) and mean patch sizes (MPS) according to seven crop classes are shown in Fig. 8a and 8b, respectively. The error bars in each figure represent the data variability of different ACP types.

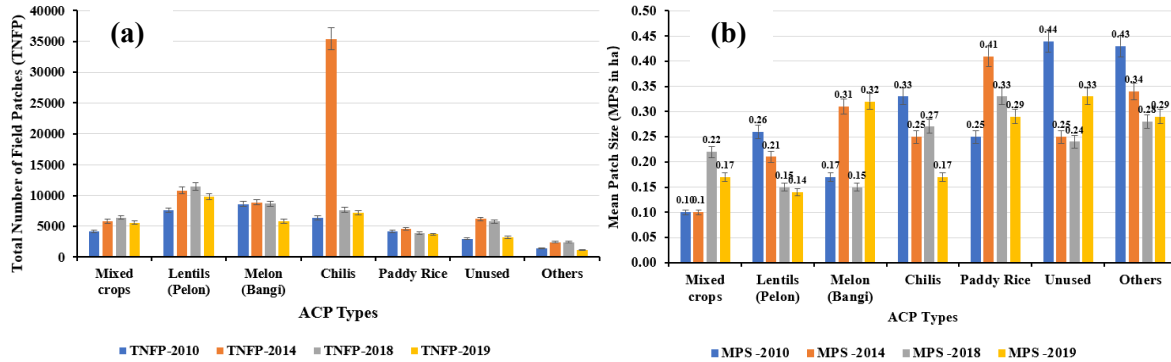


Figure 8: (a) Total number of field patches (TNFP) and (b) mean patch sizes of seven crop classes in the study area from 2010 to 2019

The number of field patches of Lentils (Pelon) were identified as highest in three years, as in 2014 (10812), 2018 (11449), and 2019 (9854) (Fig. 8a) compared to all other major crops and the MPS are 0.21 ha, 0.14 ha, and 0.15 ha, respectively (Fig. 8b). In contrast, Chilis, Paddy Rice categories are recorded as smaller number of field plots compared to Mixed crops, Lentils (Pelon) and Melon (Bangl). The MPS of major crops such as, Chilis, Paddy Rice is significantly higher in 2019 as 0.17 ha, and 0.29 ha, respectively. Conversely, the MPS of Paddy Rice is estimated lower in 2019 (0.29 ha) comparative to previous periods as estimated 0.41 in 2014, and 0.33 ha in 2018 except in 2010 (0.25 ha) (Fig. 8b). The MPS analysis suggest the spatial variation of ACP types present at field level. On the other hand, the TNFP graph (Fig. 8a) suggest that, in recent time from 2014-2019, Lentils (Pelon), Melon (Bangl), Chilis, and Mixed crops (required less water to grow) are cultivated more in winter season compared to Paddy Rice cultivation (required more water).

Crop Pattern Changing status of the study area based on different time periods

In this section, clear and legible understanding on the alteration or modification of CP area through the designated time periods are discussed. Mixed crops are mainly referred to more than one crops under cultivation. The areas of mixed crops were increased about 7.00%, while Paddy rice and Melon (Bangl) areas were also increased about 1.69%, 6.57%, respectively during 2010_{Landsat-5} to 2019_{Landsat-8}. On the other hand, all other crops were in decreased state in the same time period. The details of the changing status of CP in different time periods, such as, 2010-2014, 2014-2018, 2018-2019 and 2010-2019 is shown in Table 4 calculated based on Eq. 1 (see section 3.2.3).

Table 4: Crop pattern area changes in the study area from 2010 to 2019.

Crop Types	2010 to 2014		2014 to 2018		2018 to 2019		2010 to 2019	
	(a-b)		(b-c)		(c-d)		(a-d)	
	Change of Area (ha)	(%) Change						
Mixed crops	(+) 167.96	(+) 0.54	(+) 853.33	(+) 8.71	(-) 477.66	(-) 2.25	(+) 543.63	(+) 7.00
Lentils (pelon)	(+) 340.92	(-) 1.33	(-)577	(-) 2.33	(-) 317.92	(-) 0.62	(-) 554	(-) 4.28
Melon (Bangi)	(+) 1285	(+) 7.91	(-) 1498.55	(-) 11.73	(+) 617.67	(+) 10.39	(+) 404.12	(+) 6.57
Chilis	(+) 740.25	(+) 10.94	(+) 714.58	(+) 8.12	(-) 891.34	(-) 5.65	(-) 917.01	(-) 8.47
Paddy Rice	(+) 839.81	(+) 5.01	(-) 354.65	(-) 1.63	(-) 446.98	(-) 1.69	(+) 38.18	(+) 1.69
Unused	(+) 220	(-) 0.96	(-) 129.33	(+) 0.22	(-) 344.93	(-) 0.72	(-) 254.26	(-) 1.46
Others	(+) 198.77	(-) 0.23	(-) 141.52	(-) 0.32	(-) 232.2	(-) 0.47	(-) 174.95	(-) 1.02

Note: Positive (+) and Negative (-) data values are representing increase and decrease of an crop types area, respectively.

The rate of change yr^{-1} was positively higher (10.39%) in the Melon (Bangi) areas during 2018-2019 winter time (see Table 5) compared to 1.93% and 2.93% during 2010-2014, and 2014-2018, respectively. This change was noticed in recent time for the growing importance of Melon (Bangi) practices to support the greater number of populations in these areas, while others crops are in decreasing trends yr^{-1} . These downtrends also observed in other time periods. However, overall (2010-2019), the rate of change yr^{-1} in three different crops such as, Melon (locally known as Bangi), Mixed crops, and Paddy Rice were in positive trends as 0.73%, 0.37% and 0.19%, respectively, while others especially Chilis, Lentils (Pelon), Unused and others types were changing in downtrends as -0.94%, -0.48%, -0.16% and -0.11%, respectively (Table 5).

Table 5: Gain/Loss (%) and rate of change of crop types estimated based on different time periods data.

Crop types	2010-2014	2014-2018	2018-2019	2010-2019
Mixed crops	0.54 (0.13)	8.71 (2.18)	-2.25 (-2.25)	7.00 (0.37)
Lentils (Pelon)	-1.33 (-0.33)	-2.33 (-0.58)	-0.62 (-0.62)	-4.28 (-0.48)
Melon (Bangi)	7.91 (1.98)	11.73 (2.93)	10.39 (10.39)	6.57 (0.73)
Chilis	10.94 (2.73)	8.12 (2.03)	-5.65 (-5.65)	-8.47 (-0.94)
Paddy Rice	-5.01 (-1.25)	-1.63 (-0.41)	-1.69 (-1.69)	1.69 (0.19)
Unused	-0.96 (-0.24)	0.22 (0.05)	-0.72 (-0.72)	-1.46 (-0.16)
Others	-0.23 (-0.06)	-0.32 (-0.08)	-0.47 (-0.47)	-1.02 (-0.11)

Note: The positive and negative value refers Gain (%) and Loss (%); per year rate of change % values of all crops are shown in parenthesis.

The study further performs cross-classification in three different time periods such as 2010-2014, 2014-2018 and 2018-2019. The details of inter-conversion crop pattern changes estimated based on three different time interval data are presented in Table 6.

Table 6: Crop pattern change inter-conversion estimated based on three different time interval data (i.e., 2010-2014, 2014-2018, and 2018-2019 (area in hectare)

Time frame	Crop Class	Inter-conversion to						
		Mixed crops	Lentils (Pelon)	Melon (Bangi)	Chilis	Paddy rice	Unused	Others
2010-2014	Mixed crops	42.74	59.54	49.64	42.03	23.09	32.09	8.02
	Lentils (Pelon)	45.87	439.13	539.87	61.73	255.42	92.82	43.03
	Melon (Bangi)	46.43	160.56	202.93	241.56	74.82	232.71	39.09
	Chilis	32.39	330.43	663.87	63.79	464.19	133.72	85.47
	Paddy Rice	18.93	56.94	110.51	131.31	79.56	324.89	107.27
	Unused	12.98	131.98	289.41	26.44	467.06	111.16	145.35
	Others	7.05	19.15	43.23	16.41	108.16	131.39	222.58
2014-2018	Mixed Crops	30.84	54.91	44.81	37.35	26.03	32.79	13.54
	Lentils (Pelon)	327.01	298.63	98.00	290.93	168.12	79.35	33.54
	Melon (Bangi)	417.11	357.77	108.20	586.61	375.34	161.54	54.86
	Chilis	35.51	161.32	227.07	105.84	42.34	149.83	37.97
	Paddy Rice	239.64	158.56	48.86	487.28	327.52	183.76	96.19
	Unused	48.90	150.61	162.24	213.58	93.90	392.49	117.22
	Others	37.71	36.69	35.71	94.30	110.84	168.60	193.13
2018-2019	Mixed Crops	259.80	91.43	406.21	10.57	107.06	5.90	3.33
	Lentils (Pelon)	80.42	401.29	225.62	154.58	24.84	28.52	1.46
	Melon (Bangi)	18.56	181.32	28.18	351.17	18.33	82.17	3.28
	Chilis	86.69	178.45	677.49	151.60	306.42	175.29	5.56
	Paddy Rice	214.34	70.71	259.23	32.84	332.34	29.90	26.71
	Unused	21.67	56.24	86.75	206.20	121.53	592.55	41.58
	Others	23.44	6.34	21.05	20.19	123.26	124.38	233.30

The study result shows that in recent time (2018-2019), mixed crops and Melon (Bangi), cultivation have been decreased significantly compared to 2010-2014 time period. From this table, it is clearly evident that in 2018-2019, Unused land and others categories are also significantly decreased in the study area due to water scarcity and alternative practices, respectively compared to earlier two time periods. However, the conversion from mixed crops to Melon (Bangi) (406.21 ha) is higher compared to remaining classes at the same time period. Whereas, it is higher in Melon (Bangi) to Chilis conversion as recorded 586.61 ha during 2014-2018 (Table 6). On the other hand, during 2010-2014, Lentils (Pelon) to Melon (Bangi) conversion was observed significantly higher (539.87 ha) compared to other crop conversions (Table 6).

Crop Pattern Changes flow distribution analysis through Sankey diagram

In this study, the ACP inter-conversion flow is clearly visible through the Sankey diagram (recently adopted by Cuba, 2015) which can help to better visualize flow distribution, persistence and of ACP category in three-time window (i.e., 2010-2014, 2014-2018, and 2018-2019) (Fig. 9).

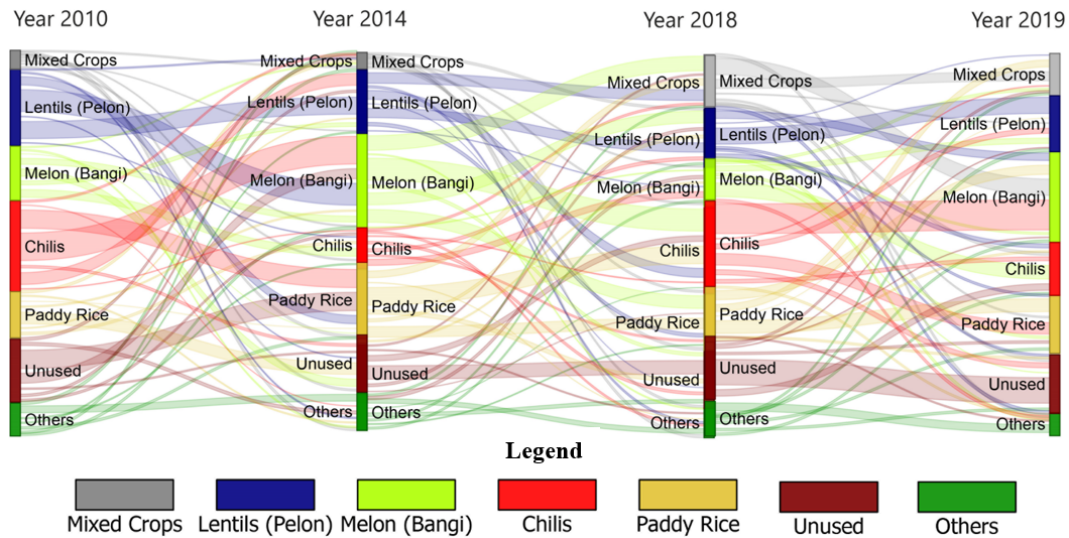


Figure 9: Sankey diagram for ACP change flow distribution based on three-time window (i.e., 2010-2014, 2014-2018, and 2018-2019).

The diagram is comprised of four vertical stacked bars and three sets of persistence and transition flow lines are positioned between each chronological sequential pair of vertical stacked bar (i.e., initial time t_1 and a subsequent time t_2), based on the data generated in Table 6. The flow line thickness in each category is proportional to the size of the particular crop area that ideally represented the corresponding persistence or transition. The line colors for each category in vertical bar are assigned based on the seven classes color code legend similar to the ACP maps color code (see Fig. 7). The respective flow line color is assigned at the initial category at time t_1 . Similarly other time periods also completed based on the same color code.

Overall assessment

In general, the eight or more years of observations are absolutely necessary to find out the trend of changing crop pattern in any study area, and this has been reported clearly in the research conducted by Waldhoff *et al.*, (2017) focused on Rur catchment area, Germany. Therefore, in our study, we have considered 10 years of observations time period started from 2010 to 2019. Among all the years, some year shows increasing and some representing decreasing trends. The overall assessment results clearly demonstrated that Mixed Crop cultivation is practiced in both Upazilas (i.e., Hathazari and Raozan), and shows increasing trend during 2010 to 2019 as 207.45 ha (7.26%) and 336.18 ha (6.88%), respectively. Lentils (Pelon) was identified as the most common crop and observed 271.79 ha and 282.21 ha in Hathazari and Raozan Upazilas, respectively. This has been practiced in the specific areas

where less water available during winter season. The rate of this cultivation is in declining state due to preferences of other crops. On the other hand, Melon (Bangi) cultivation was also dominated at certain extent during this time period. Paddy Rice is the main crop considered and cultivated in Bangladesh, but in the study area, this practice was found less compared to other crops.

The non-availability of agricultural records at sub-district level is identified as the major drawbacks in the agricultural research in Bangladesh. To maintain the growing demand of agricultural crop production, it is necessary to know the actual crop statistics for the particular year or even the previous years. Hence, scientific reliable information is required to know exactly what type of crops are grown where.

The uneven ACP and different types of crop production at regional, national and global level makes this task difficult and challenging to compare. In recent time (year 2017), cropping systems diversity of 42 Upazilas of Chittagong region during 2016 was assessed by Shahidullah *et al.*, (2017) and observed 93 cropping patterns, where eight cropping patterns existed with rice crop covers, 19 cropping patterns with non-rice, and rest 66 are by rice-non rice patterns. But no statistics is separable as it contained the year-round practices result of the year 2014-2015. In addition, Congalton, (1991) studied different crop practices (i.e., Coconut plantation, Ragi, Rice, Maize and Wheat) in Tumkur taluk area of Tumkur district in Karnataka, India which required less maintenance and less water that can adapt the changing climatic conditions.

The derived crop statistics in our study doesn't match or compared with other databases such as National Agricultural Yearbook (NAY) which prepared at district level without considering satellite datasets. Therefore, in this regard, our Landsat derived crop results will fulfill the data gaps in the study regions which can be implemented in other sub-district areas also for crop pattern identification and change mapping.

Conclusion and Future directions

The study first time focused on the changing landscape of Hathazari and Raozan upazila in South-eastern region, Bangladesh to identify ACP and its historical changes from 2010 to 2019 time periods. The information extraction on ACP at sub-district level is critically important as the study area running with water shortage in wintertime which confirmed by satellite-based precipitation data records represented in Fig. 2. The study utilized unsupervised classification technique to detect variety of crop pattern and their changes at sub-district level especially in Hathazari and Raozan Upazilas. In this study, Landsat 5 TM and Landsat 8 OLI sensors temporal data (30 m resolution) served as basic data input for CP identification, mapping and change analysis with good accepted accuracy results which satisfied our first objective. This first objective achieved the goal as the unsupervised K-means clustering classification algorithm successfully identified the seven ACP types, which are separated from agricultural land that originally derived from the LU classified maps of the same time frame. The maps are validated with the field GPS data as ground truth, GE high resolution images, ESRI World Wayback imagery, and random points generated based on the classified image considered for accuracy assessment. Considering all four years (i.e., 2010, 2014, 2018, and 2019), the UA and PA of the important major classes (i.e., Mixed crops, Lentils, Melon, Chilis and Paddy Rice) were observed within the range of 66.67-97.83% and 87.50-96.55%, respectively. The overall accuracies and the Kappa coefficients in the CP in 2010, 2014, 2018, and 2019 are as 81.13%, 86.79%, 76.89%, 83.02% and 0.78,

0.84, 0.73, and 0.80, respectively. Moreover, the estimated (four-year average) overall accuracy and kappa coefficient values were achieved 81.96% and 0.79, respectively. The images were considered in this study are cloud free, therefore uncertainty is minimized at certain extent and the data quality is assured in this regard. Moreover, in other perspective, few uncertainties existed in the selective crop classes which can be identified through the accuracy assessment and error matrices table. More number of ground truth validation points and more reference point's generation can improve the classification accuracy at the individual class label.

The retrieved data has great potential to provide reliable, and robust for further consideration in future ACP mapping. The results found robust in ACP identification and observed significant variations in crops at sub-district level. The resultant maps can identify the spatio-temporal variations of ACP derived from AGL images and according to classes, statistical comparison was made based on the temporal change analysis in four-time domain (2010, 2014, 2018 and 2019) that helped us to achieve our second objective. Finally, the study analyzed the ACP dynamics, persistence and change in three-time intervals as, 2010-2014, 2014-2018, and 2018-2019 based on the class wise inter-conversion assessment, and the changes are finalized through cross-tabulation matrices. Moreover, these changes are better illustrated and visualized through Sankey diagram which satisfied our third objective.

Based on this ACP statistics information, government should collect data at sub-district level which can help them to maintained crop records at regular basis. To support the Government of Bangladesh (GoB), sustainable agricultural crop practices and its pattern identification including crop statistics is very much required to achieve the UN Sustainable Development Goals (SDGs). By observing the data gap in the present study, it creates a window to work on this topic further, which have a greater importance to create a digital record of the agricultural statistics required for crop management and sustainable agricultural development in this area. The existing database queried through simple SQL statement within the ArcGIS 10.8 software platform can be effective for future crop monitoring. Moreover, the database update work for the same region, as well as particular policy can be adopted at an earliest based on the multiple crop pattern information. The study areas are largely practiced mixed crops cultivation, Lentils (Pelon) and Melon (Bangi) as these are required less water to grow, compared to Paddy Rice cultivation. Moreover, the study further suggests to consider high resolution Sentinel-2 MSI, and Gaofen-2 MSI satellite images for future ACP mapping in this area with greater accuracy.

References

- Atzberger, C., (2013). Advances in remote sensing of agriculture: context description, existing operational monitoring systems and major information needs. *Remote Sensing* 5(2), 949-981.
- Belgiu, M., & Csillik, O., (2018). Sentinel-2 cropland mapping using pixel-based and object-based time-weighted dynamic time warping analysis. *Remote Sensing of the Environment*, 204, 509–523. <https://doi.org/10.1016/j.rse.2017.10.005>
- Bhuiyan, M.M.H., Islam, K., Islam, K.N., & Jashimuddin, M., (2019). Monitoring dynamic land-use change in rural–urban transition: a case study from Hathazari Upazila, Bangladesh. *Geology, Ecology, and Landscapes*, 3(4), 247-257. <https://doi.org/10.1080/24749508.2018.1556034>

- Brammer, H., (1996). The geography of the Soils of Bangladesh. University Press Limited, Dhaka, Bangladesh
- Casasnovas, J.M., Montero, A.M., & Casterad, M.A., (2005). Mapping multi-year cropping patterns in small irrigation districts from timeseries analysis of Landsat TM images. *European Journal of Agronomy*, 23(2), 159-169.
- Congalton, R.G., (1991). A review of assessing the accuracy of classifications of remotely sensed data. *Remote Sensing of the Environment*, 37, 35-46.
- Congalton, R.G., & Green, K., (2008). *Assessing the Accuracy of Remotely Sensed Data: Principles and Practices*, 2nd Ed. CRC Press.
- Conrad, C., Fritch, S., Zeidler, J., Rucker, G., & Dech, S., (2010). Per-field irrigated crop classification in arid Central Asia using SPOT and ASTER data. *Remote Sensing*, 2(4), 1035-1056.
- Cohen, J., (1960). A coefficient of agreement of nominal scales. *Educational and Psychological Measurements*, 20(1), 37-46.
- Cuba, N., (2015). Research note: Sankey diagrams for visualizing land cover dynamics. *Landscape and Urban Planning* 139, 163-167.
- Garcia, A.S., De F.N. Vilela, V.M., Rizzo, R., West, P., Gerber, J.S., Engstrom, P.M., & Ballester, M.V.R., (2019). Assessing land use/cover dynamics and exploring drivers in the Amazon's arc of deforestation through a hierarchical, multi-scale and multi-temporal classification approach. *Remote Sensing Applications: Society and Environment*, 15, 100233. <https://doi.org/10.1016/j.rsase.2019.05.002>
- Feng, S., Zhao, J., Liu, T., Zhang, H., Zhang, Z., & Guo, X., (2019). Crop type identification and mapping using machine learning algorithms and Sentinel-2 time series data. *IEEE Journal of Selected Topics in Applied Earth Observations and Remote Sensing*, 12(9), 3295–3306.
- Foley, J.A., Ramankutty, N., Brauman, K.A., Cassidy, E.S., Gerber, J.S., Johnston, M., ... & Zaks, D.P.M., (2011). Solutions for a cultivated planet. *Nature*, 478, 337–342. <https://doi.org/10.1038/nature10452>
- Fritz S., See, L.M., You, L., Justice, C., Becker-Reshef, I., Bydekerke, L., ... & Woodcock, C., (2013). The Need for Improved Maps of Global Cropland. *Eos Transactions*, 94(3), 31-32. <http://dx.doi.org/10.1002/2013EO030006>
- Hill, M.J., Ticehurst, C.J., Lee, J.-S., Grunes, M.R., Donald, G.E., & Henry, D., (2005). Integration of Optical and Radar Classifications for Mapping Pasture Type in Western Australia. *IEEE Transaction in Geosciences and Remote Sensing*, 43(7), 1665–1681.
- Hong, G., Zhang, A., Zhou, F., & Brisco, B., (2014). Integration of Optical and Synthetic Aperture Radar (SAR) Images to Differentiate Grassland and Alfalfa in Prairie Area. *International Journal of Applied Earth Observation and Geoinformatics*, 28, 12–19. <https://dx.doi.org/10.1016/j.jag.2013.10.003>
- Hong, G., Zhang, A., Zhou, F., Townley-Smith, L., Brisco, B., & Olthof, I., (2011). Crop-Type Identification Potential of Radarsat-2 and MODIS Images for the Canadian Prairies. *Canadian Journal of Remote Sensing*, 37(1):45–54.
- Huq, S.M., & Shoaib J., (2013). The Soils of Bangladesh. Springer Science+Business Media LLC, New York, United States
- Islam, K., Jashimuddin, M., Nath, B., & Nath, T.K., (2018). Land use classification and change detection by using multi-temporal remotely sensed imagery: The case of Chunati wildlife sanctuary, Bangladesh. *The Egyptian Journal of Remote Sensing and Space Science* 21(1), 37–47. <https://doi.org/10.1016/j.ejrs.2016.12.005>

- Jain, M., Mondal, P., DeFries, R.S., Small, C., & Galford, G.L., (2013). Mapping cropping intensity of smallholder farms: A comparison of methods using multiple sensors. *Remote Sensing of the Environment*, 134, 210–223.
- Justice, C.O., & Becker-Reshef, I., 2007. Developing a Strategy for Global Agricultural Monitoring in the Framework of Group on Earth Observations (GEO). Report from the Workshop, July. UN FAO. https://www.earthobservations.org/documents/cop/ag_gams/200707_01/20070716_geo_igol_ag_workshop_report.pdf
- Liaghat, S., & Balasundram, S.K., (2010). A Review: The Role of Remote Sensing in Precision Agriculture. *American Journal of Agricultural and Biological Sciences*. 5(1), 50-55. <https://doi.org/10.3844/AJABSSP.2010.50.55>
- Long, J.A., Lawrence, R.L., Greenwood, M.C., Marshall, L., & Miller, P.R., (2013). Object oriented crop classification using multitemporal ETM+ SLC-off imagery and random forest. *GIScience & Remote Sensing* 50(4), 418-436.
- Liu, J., Liu, M., Tian, H., Zhuang, D., Zhang, Z. & Deng, X., (2005). Spatial and temporal patterns of China's cropland during 1990-2000: an analysis based on Landsat TM data. *Remote Sensing of the Environment*, 98:442-456.
- Liu, Y., Song, W., & Deng, X., (2016). Changes in crop type distribution in Zhangye City of the Heihe River Basin, China. *Applied Geography*, 76, 22-36.
- Mingwei, Z., Qingbo, Z., Zhongxin, C., Jia, L., Yong, Z., & Chongfa C., (2008). Crop discrimination in Northern China with double cropping systems using Fourier analysis of time-series MODIS data. *International Journal of Applied Earth Observation and Geoinformatics*. 2008, 10(4), 476–485. <https://doi.org/10.1016/j.jag.2007.11.002>
- Murakami, T., Ogawa, S., Ishitsuka, N., Kumagai, K., & Saito, G., (2001). Crop discrimination with multitemporal SPOT/HRV data in the Saga plains, Japan. *International Journal of remote Sensing*, 22, 1335-1348.
- Nellis, M.D., Price, K.P., & Rundquist, D., (2009). Remote Sensing of Cropland Agriculture. Papers in Natural Resources. Paper 217. University of Nebraska–Lincoln Publication: Lincoln, NE, USA. <https://doi.org/10.4135/9780857021052.n26>
- Odenweller, J.B., & Johnson, K.I., (1984). Crop identification using Landsat temporal spectral profiles. *Remote Sensing of the Environment*, 14,39-54. [https://doi.org/10.1016/0034-4257\(84\)90006-3](https://doi.org/10.1016/0034-4257(84)90006-3)
- Okamoto, K., (1999). Estimation of Rice-Planted Area in the Tropical Zone Using a Combination of Optical and Microwave Satellite Sensor Data. *International Journal of Remote Sensing*, 20 (5), 1045–1048. <https://doi.org/10.1080/014311699213091>
- Ozdogan, M., (2010). The spatial distribution of crop types from MODIS data: temporal unmixing using Independent Component Analysis. *Remote Sensing of the Environment*, 114, 1190–1204. <https://doi.org/10.1016/j.rse.2010.01.006>
- Panigrahy, S., & Sharma, S.A., (1997). Mapping of crop rotation using multirate Indian Remote Sensing Satellite digital data. *ISPRS Journal of Photogrammetry and Remote Sensing*, 52, 85–91.
- Panigrahy, S., Singh, R.P., Sharma, S.A., & Chakraborty, M., (1995). Results of potential use of simulated IRS-1C WiFS data for crop monitoring. *Journal of the Indian Society of Remote Sensing* 23,175-185. <http://dx.doi.org/10.1007/BF03024498>
- Pradhan, S., (2001). Crop area estimation using GIS, remote sensing and area frame sampling. . *International Journal of Applied Earth Observation and Geoinformatics* 3(1), 86–92.

- Quarmby, N.A., Townshend, J.R.G., Settle, J.J., White, K.H., Milnes, M., Hindle, T.L., & Silleos, N., (1992). Linear mixture modelling applied to AVHRR data for crop area estimation. *International Journal of Remote Sensing*, 13(3), 415-425.
- Rahman, M.R., & Saha, S.K. (2009). Spatial Dynamics of Cropland and Cropping Pattern Change Analysis Using Landsat TM and IRS P6 LISS III Satellite Images with GIS. *Geo-spatial Information Science*, 12(2):123-134. <https://doi.org/10.1007/s11806-009-0249-2>
- Ray, S.S., Sood, A., Das, G., Panigrahy, S., Sharma, P.K., & Prihar, J.S., (2005). Use of GIS and Remote Sensing for crop diversification- A case study for Punjab State. *Journal of the Indian Society of Remote Sensing*, 33(2), 181-188. <https://doi.org/10.1007/BF02990034>
- Santanu, P., Chakrabarty, A., & Bhadury, S., (2014). Application of Remote Sensing & GIS in Crop Information System – a case study of Paddy monitoring in Jamalpur Block. *IOSR Journal of Agriculture and Veterinary Science (IOSR-JAVS)*, 6(6), 45-51. <https://iosrjournals.org/iosr-javs/papers/vol6-issue6/I0664551.pdf>
- Shahidullah, S.M., Nasim, M., Quais, M.K., & Saha, A., (2017). Diversity of Cropping Systems in Chittagong Region. *Bangladesh Rice Journal*, 21(2):109-122. https://brri.portal.gov.bd/sites/default/files/files/brri.portal.gov.bd/page/9f8ef38c_8bd5_4bd3_a786_c064aed9bb7b/Article_5_21_2.pdf.
- Singh, S., (1980). Dynamics of cropping pattern in northern India: Perspectives in agricultural geography. Concept Publishing Company, New Delhi, India.
- Singh, N.J., Kudrat, M., Jain, K., & Pandey, K., (2011). Cropping pattern of Uttar Pradesh using IRS-P6 (AWiFS) data. *International Journal of Remote Sensing*, 32(16), 4511-4526. <https://doi.org/10.1080/01431161.2010.489061>
- Thenkabail, P.S., (2010). Global Croplands and their Importance for Water and Food Security in the Twenty-first Century: Towards an Ever Green Revolution that Combines a Second Green Revolution with a Blue Revolution. *Remote Sensing*, 2(9), 2305-2312. <https://doi.org/10.3390/rs2092305>
- Tian, H., Wu, M., Wang, L., & Niu, Z., (2018). Mapping Early, Middle, and Late Rice Extent Using Sentinel-1A and Landsat-8 Data in the Poyang Lake Plain, China. *Sensors*, 18,185. <https://doi.org/10.3390/s18010185>
- Waldhoff, G., Curdt, C., Hoffmeister, D., & Bareth, G., (2012). Analysis of multitemporal and multi-sensor remote sensing data for crop rotation mapping. *ISPRS Annals of the Photogrammetry, Remote Sensing and Spatial Information Sciences*, 1-7,177-182.
- Waldhoff, G., Lussem, U., & Bareth, G. (2017). Multi-Data Approach for remote sensing-based regional crop rotation mapping: A case study for the Rur catchment, Germany. *International Journal of Applied Earth Observation and Geoinformation*, 61, 55-69. <https://doi.org/10.1016/j.jag.2017.04.009>
- Waldner, F., Canto, G.S., & Defourny, P., (2015). Automated annual cropland mapping using knowledge-based temporal features. *ISPRS Journal of Photogrammetry and Remote Sensing*, 110:1-13.
- Wang, S., Azzari, G., & Lobell, D.B., (2019). Crop type mapping without field-level labels: Random forest transfer and unsupervised clustering techniques. *Remote Sensing of the Environment*, 222,303-317. <https://doi.org/10.1016/j.rse.2018.12.026>
- Wardlow, B.D., & Egbert, S.L., (2008). Large-area crop mapping using time-series MODIS 250 m NDVI data: An assessment for the U.S. Central Great Plains. *Remote Sensing of the Environment*, 112(3),1096-1116. <https://doi.org/10.1016/j.rse.2007.07.019>

- Whitcraft, A.K., Vermote, E.F., Becker-Reshef, I., & Justice, C.O., (2015). Cloud cover throughout the agricultural growing season: Impacts on passive optical earth observations. *Remote Sensing of the Environment* 156,438–447
- Wu, B., Gommers, R., Zhang, M., Zeng, H., Yan, N., Zou, W. & Van Heijden, A., (2015). Global crop monitoring: a satellite-based hierarchical approach. *Remote Sensing* 7(4), 3907-3933. <https://doi.org/10.3390/rs70403907>
- Yu, K., Li, F., Gnyp, M.L., Miao, Y., Bareth, G., & Chen, X., (2013). Remotely detecting canopy nitrogen concentration and uptake of paddy rice in the Northeast China Plain. *ISPRS Annals of the Photogrammetry, Remote Sensing and Spatial Information Sciences*, 78,102–115. <https://doi.org/10.1016/j.isprsjprs.2013.01.008>

Appendix A. 1-2. Supplementary files:*Table A.1 Categories wise land use distribution of the study area from 2010 to 2019*

LU categories	2010		2014		2018		2019	
	Area (ha)	Area (%)	Area (ha)	Area (%)	Area (ha)	Area (%)	Area (ha)	Area (%)
Agricultural land	9282.17	19.85	11594.38	24.80	10461.08	22.37	8367.48	17.90
Settlement with vegetation	11803.39	25.24	13706.03	29.31	14575.51	31.17	14125.60	30.21
Hill Forest	6665.43	14.26	7209.01	15.41	8983.81	19.21	9329.82	19.95
Barren land	10250.16	21.92	10017.44	21.42	9329.53	19.95	10855.04	23.22
Water Bodies	8756.31	18.73	4230.77	9.04	3347.97	7.16	4079.87	8.72
Total	46757.45	100	46757.45	100	46757.45	100	46757.45	100

Source: USGS Landsat satellite data from 2010 to 2019 and ENVI 5.3 and ArcGIS 10.7 software.

Table A.2 Classification accuracy assessment of 2010, 2014, 2018, and 2019 LU image classified results

(A) 2010		Accuracy matrix					Classification accuracy				
LU Types	Ag	Sv	Hf	Bl	Wb	Total	Pa (%)	Ua (%)	Oa (%)	Kappa	
Ag	11	0	0	1	2	13	55.00	84.61	74.67	0.67	
Sv	5	37	1	1	1	45	82.22	82.22			
Hf	2	5	18	5	0	30	90.00	60.00			
Bl	2	2	1	26	4	35	68.42	74.29			
Wb	0	1	0	6	20	27	74.07	74.07			
Total	20	45	20	38	27	150					

(b) 2014		Accuracy matrix					Classification accuracy				
LU Types	Ag	Sv	Hf	Bl	Wb	Total	Pa (%)	Ua (%)	Oa (%)	Kappa	
Ag	10	0	0	2	1	13	58.82	76.92	76.67	0.70	
Sv	5	36	2	2	0	45	83.72	80.00			
Hf	0	4	23	2	1	30	88.46	76.67			
Bl	2	2	0	22	9	35	75.86	62.86			
Wb	0	1	1	1	24	27	68.57	88.89			
Total	17	43	26	29	35	150					

(c) 2018		Accuracy matrix					Classification accuracy				
LU Types	Ag	Sv	Hf	Bl	Wb	Total	Pa (%)	Ua (%)	Oa (%)	Kappa	
Ag	10	1	0	1	1	13	66.67	76.92	71.33	0.63	
Sv	3	39	1	2	0	45	78.00	86.67			
Hf	0	8	21	1	0	30	70.00	70.00			
Bl	1	2	6	17	9	35	68.00	48.57			
Wb	1	0	2	4	20	27	66.67	74.07			
Total	15	50	30	25	30	150					

(d) 2019		Accuracy matrix					Classification accuracy				
Lu Types	Ag	Sv	Hf	Bl	Wb	Total	Pa (%)	Ua (%)	Oa (%)	Kappa	
Ag	10	1	2	0	0	13	90.91	76.92	82.00	0.77	
Sv	0	41	3	0	1	45	82.00	91.11			
Hf	0	7	19	0	4	30	76.00	63.33			
Bl	0	1	1	28	5	35	96.55	80.00			
Wb	1	0	0	1	25	27	71.43	92.59			
Total	11	50	25	29	35	150					

Appendix B. Supplementary files:

Table B- Classification accuracy assessment and confusion error matrix information based on 2010, 2014, 2018, and 2019 CP classified image results.

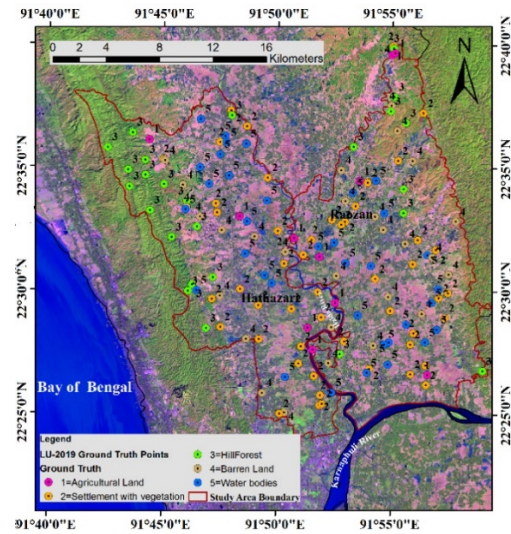
(a) 2010		IMAGE CLASSIFIED DATA									ERRORS OF OMISSION (%)
CROP TYPES	MC	LP	MB	CH	PR	UU	OT	TOTAL	PA (%)		
GROUND TRUTH REFERENCE DATA	MC	21	2	1	1	0	0	1	26	77.78	19.33
	LP	4	30	1	1	1	0	1	38	83.33	21.05
	MB	0	3	39	1	4	1	2	50	88.64	22.00
	CH	0	0	1	28	1	1	1	32	87.50	12.50
	PR	0	0	1	0	25	2	0	28	71.43	10.71
	UU	2	0	1	0	4	21	0	28	84.00	25.00
	OT	0	1	0	1	0	0	8	10	61.54	20.00
TOTAL	27	36	44	32	35	25	13	212	OA (%)	81.13	
UA (%)	80.77	78.95	78.00	87.50	89.29	75.00	80.00		KAPPA	0.78	
ERRORS OF COMMISSION (%)	22.22	16.67	11.36	12.50	28.57	16.00	38.46				

(b) 2014		IMAGE CLASSIFIED DATA									ERRORS OF OMISSION (%)
CROP TYPES	MC	LP	MB	CH	PR	UU	OT	TOTAL	PA (%)		
GROUND TRUTH REFERENCE DATA	MC	21	1	1	1	0	1	1	26	91.30	19.23
	LP	2	34	0	1	1	0	0	38	89.47	10.53
	MB	0	1	45	2	0	2	0	50	97.83	10.00
	CH	0	0	0	28	1	2	1	32	84.85	12.50
	PR	1	1	0	1	23	2	0	28	82.14	17.86
	UU	0	1	0	0	2	24	1	28	85.71	14.29
	OT	0	0	0	0	0	1	9	10	10.00	10.00
Total	24	38	46	33	27	32	12	212	OA (%)	86.79	
UA (%)	87.50	89.47	97.83	84.85	85.18	75.00	75.00		KAPPA	0.84	
ERRORS OF COMMISSION (%)	12.50	10.53	2.17	15.15	14.81	25.00	25.00				

(c) 2018		IMAGE CLASSIFIED DATA								
-----------------	--	-----------------------	--	--	--	--	--	--	--	--

		CROP TYPES	MC	LP	MB	CH	PR	UU	OT	TOTAL	PA (%)	ERRORS OF OMISSION (%)
GROUND TRUTH REFERENCE DATA	MC	21	2	1	0	0	2	0	26	80.77	19.23	
	LP	4	30	0	1	2	1	0	38	78.95	21.05	
	MB	2	3	38	0	4	3	0	50	76.00	24.00	
	CH	0	0	1	28	0	1	2	32	87.50	12.50	
	PR	0	0	0	0	20	3	5	28	71.43	28.57	
	UU	0	2	0	0	4	20	2	28	71.43	28.57	
	OT	0	0	4	0	0	0	6	10	60.00	40.00	
Total		27	37	44	29	30	30	15	212	OA (%) 76.89		
UA (%)		77.78	81.08	86.36	96.55	66.67	66.67	40.00		KAPPA 0.73		
ERRORS OF COMMISSION (%)		22.22	18.92	13.64	3.45	33.33	33.00	60.00				
(d) 2019												
IMAGE CLASSIFIED DATA												
		CROP TYPES	MC	LP	MB	CH	PR	UU	OT	TOTAL	PA (%)	ERRORS OF OMISSION (%)
GROUND TRUTH REFERENCE DATA	MC	23	1	1	0	0	1	0	26	88.46	11.54	
	LP	3	31	0	1	2	1	0	38	81.58	18.42	
	MB	1	3	40	0	3	3	0	50	80.00	20.00	
	CH	0	0	1	29	0	1	1	32	90.62	9.38	
	PR	0	0	0	0	22	3	3	28	78.57	21.43	
	UU	2	2	0	0	3	21	2	28	75.00	25.00	
	OT	0	0	0	0	0	0	10	10	100.00	0.00	
Total		27	37	42	30	30	30	16	212	OA (%) 83.02		
UA (%)		85.18	78.95	78.00	87.50	89.29	75.00	80.00		KAPPA 0.80		
ERRORS OF COMMISSION (%)		22.22	16.67	11.36	12.50	28.57	16.00	38.46				

Appendix B. Fig. 1 Supplementary file:



Supplementary Fig. 1: LU ground truth collection points; 1-5 represents five different LU classes identified at field level

Appendix B. Fig. 2 Supplementary file:



Supplementary Fig. 2: Sample reference ESRI World Imagery Wayback of 31 Jan 2019 with random points for CP and LU

Reference Imagery Source:

<https://livingatlas.arcgis.com/wayback/?active=17677&ext=91.24115,22.47661,92.05551,22.89853&selected=11060>